Available online at www.sciencedirect.com
ScienceDirect
Energy Procedia 74 (2015) 211 – 225
Energy Procedia

Adaptive Fuzzy Gain Scheduling of PI Controller for control of the Wind Energy Conversion Systems

Khouloud Bedoud[a,b]*, Mahieddine Ali-rachedi[c], Tahar Bahi[d], Rabah Lakel[a]

[a] *Automatic Laboratory and Signals, Badji Mokhtar University, Annaba, Algeria.*
[b] *Welding and NDT Research Centre (CSC). BP 64 Cheraga, Algeria.*
[c] *Preparatory School in Sciences and Technics, Annaba, Algeria.*
[d] *Electrical department, Badji Mokhtar University, Annaba,Box 12, 2300 Algeria.*

Abstract

In this work, the Wind Energy Conversion Systems (WECS) based on doubly fed induction generator (DFIG) model is built. First, we consider the vector control strategy of the active and reactive powers in order to ensure an optimum operation. The whole system is presented in d-q-synchronous reference frame. After, the design of Adaptive Fuzzy Gain Scheduling of Proportional Integral Controller (AFGPI) for WECS is described, where the optimization by Fuzzy rules is utilized online to adjust the parameters of PI controller based on the error and its first derivative. Finally, the control of the active and reactive power using fuzzy-PI controller is simulated using software Matlab/Simulink, studies on a 1.5 MW DFIG wind generation system compared with conventional proportional integral controller. Performance and robustness results obtained are presented and analyzed.

Peer-review under responsibility of the Euro-Mediterranean Institute for Sustainable Development (EUMISD)

Keywords: wind systems, doubly fed induction generator, fuzzy control, fuzzy gain scheduling control, fuzzy PI control, PI controller.

* Corresponding author. Tel.: +213-388-759-82; fax: +213-388-760-05
E-mail address: k.bedoud@csc.dz

Peer-review under responsibility of the Euro-Mediterranean Institute for Sustainable Development (EUMISD)
doi:10.1016/j.egypro.2015.07.580

1. Introduction

Nowadays, there is a growing demand for renewable energy to generate electricity in order to avoid environmental issues derived from the exploitation of fossil fuels (oil, gas, coal). Wind power is one of the cleanest sources of renewable energy that allow producing the green energy. The wind generation system based on a doubly fed induction generator (DFIG) is employed widely in large wind farms that have many advantages: very high energy efficiency, robust sensorless operation [1-2] as well as easy exploitation and control [3]. In addition, the power converter is usually rated at 25-30% of the generator power rating [4-7]. For such several advantages, this machine has generated a lot of curiosity on the part of researchers who have tried to develop strategies to better exploitation of strong points [8].

The conventional proportional integral controller (PI) is widely used in the control of DFIG because of its simple structures and good performances. The problem that arises with the PI controller is that his parameters are initially calculated according to the DFIG parameters. But in practice, the machine parameters change inevitably during the time. To overcome the disadvantages this paper proposes a combination between fuzzy logic and PI controller, where the PI parameters can be adjusted online by an adaptive mechanism based on a fuzzy logic. A parameter adjustment method of PI controller with fuzzy logic was developed and used to find the optimal values of PI parameters. The simulation results show that the proposed controller provides better performance and good robustness compared with conventional PI controller.

The paper is organized as follows. Section 2, describes the modeling studied system. The various control algorithms for optimal turbine operation and control of active and reactive power will be presented in section 3. The synthesis of the two controllers and their performance are compared in section 4. The results of simulations obtained are presented and discussed for validating the proposed controller in Section 5. Finally, a conclusion is drawn in section 6.

Nomenclature

P_s, Q_s	stator active and reactive power	ωs, ωr	synchronous and rotor angular frequency
P_r, Q_r	rotor active and reactive power	ρ	air density
T_{em}	DFIG electromagnetic torque (N m)	V	wind speed
d, q	synchronous reference frame index	R	rotor radius
$V_{sd,q}$	stator d–q frame voltage	λ	tip-speed ratio
$V_{rd,q}$	rotor d–q frame voltage	Ω_{tur}	aeroturbine rotor speed
$i_{sd,q}$	stator d–q frame current	Ω_m	generator speed
$i_{rd,q}$	rotor d–q frame current	G	gearbox ratio
$\varphi_{\mathrm{sd,q}}$	stator d–q frame flux	J	turbine total inertia
$\varphi_{\mathrm{rd,q}}$	rotor d–q frame flux	J_{tur}, J_{gen}	rotor and DFIG inertia
R_s, R_r	stator and rotor Resistances	f	turbine total external damping
L_s, L_r	stator and rotor self Inductances	σ	Coefficient of dispersion.
L_{m}	mutual inductance	CNV1/CNV2	First converter/Second converter

2. Wind Turbine System Modeling

The studied system shown in Fig.1 is constituted of the turbine, the gearbox and the DFIG. The DFIG is connected directly to the grid via its stator but also via its rotor by means of the static converters to allow an exchange of energy between the network and the DFIG at the speed of synchronism. The two converters, network side and DFIG side, are controlled by Pulse Width Modulation (PWM) [9]. Through the bidirectional static converters, the DFIG can work in sub-synchronous and super-synchronous modes. Since the converters are designed for a power of 25-30% of the nominal power of the DFIG [10].

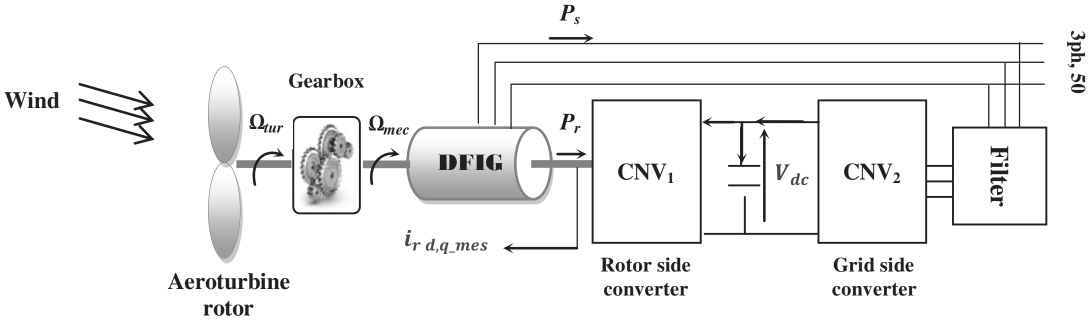

Fig. 1. Schematic diagram of DFIG wind turbine

2.1. Turbine Modeling

The theoretical power produced by the wind is given by [11-13]:

$$P_{tur} = C_p . \frac{\rho.S.V^3}{2} \tag{1}$$

Where C_p denotes power coefficient of wind turbine, its evolution depends on the blade pitch angle (β) and the tip-speed ratio (λ) which is defined as [14]:

$$\lambda = \frac{R.\Omega_{tur}}{V} \tag{2}$$

From summaries achieved on a wind of 1.5 MW, the expression of the power coefficient for this type of turbine can be approximated by the following equation [15, 16]:

$$C_p = \left(0.45 - \left(0.0167(\beta - 2)\right)\right)\left(\sin\left(\frac{\pi(\lambda+0.1)}{\left(15.5-\left(0.3(\beta-2)\right)\right)}\right)\right) - \left(0.00184(\lambda - 3)(\beta - 2)\right) \tag{3}$$

Fig. 2 illustrates the variation of the power coefficient (C_p) versus the tip-speed ratio (λ) for the value of the pitch angle β=2°. This figure indicates that there is one specific point (λ_{opt}, C_{popt}) at which the turbine is most efficient for β=2°.

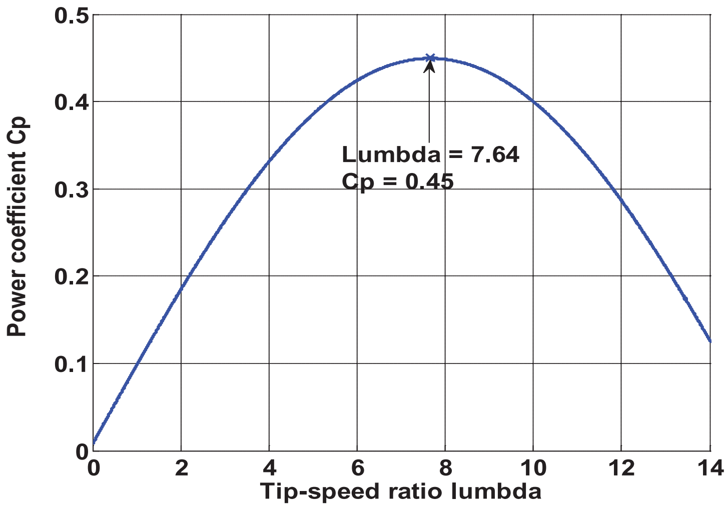

Fig. 2 Power coefficient versus tip speed ratio

The aerodynamic torque expression is given by [14]:

$$T_{tur} = \frac{P_{tur}}{\Omega_{tur}} = C_p . \frac{\rho.S.V^3}{2} . \frac{1}{\Omega_{tur}} \quad (4)$$

The gearbox is installed between the turbine and the generator to adapt the turbine speed to that of the generator:

$$\Omega_{mec} = G.\Omega_{tur} \quad (5)$$

The friction, elasticity and energy losses in the gearbox are neglected.

$$G = \frac{T_{tur}}{T_{mec}} \quad (6)$$

The mechanical equations of the system can be characterized by:

$$J\frac{d\Omega_{mec}}{dt} = T_{mec} - T_{em} - f\Omega_{mec} \quad (7)$$

With, $J = \frac{J_{tur}}{G^2} + J_{gen}$

2.2. Modeling the DFIG with stator field orientation

The Park model of DFIG is given by the equations below [16-19]:

$$\begin{cases} V_{sd} = R_s i_{sd} + \frac{d\varphi_{sd}}{dt} - \omega_s \varphi_{sq} \\ V_{sq} = R_s i_{sq} + \frac{d\varphi_{sq}}{dt} + \omega_s \varphi_{sd} \end{cases} \quad (8)$$

$$\begin{cases} V_{rd} = R_r i_{rd} + \frac{d\varphi_{rd}}{dt} - \omega_r \varphi_{rq} \\ V_{rq} = R_r i_{rq} + \frac{d\varphi_{rq}}{dt} + \omega_r \varphi_{rd} \end{cases} \quad (9)$$

As the d and q axis are magnetically decoupled, the stator and rotor flux are given as:

$$\begin{cases} \varphi_{sd} = L_s i_{sd} + L_m i_{rd} \\ \varphi_{sq} = L_s i_{sq} + L_m i_{rq} \end{cases} \quad (10)$$

$$\begin{cases} \varphi_{rd} = L_r i_{rd} + L_m i_{sd} \\ \varphi_{rq} = L_r i_{rq} + L_m i_{sq} \end{cases} \quad (11)$$

With: $L_s = L_{fs} + L_m$

$L_r = L_{fr} + M^2 L_m$

The active and reactive powers are defined as:

$$\begin{cases} P_s = V_{sd} i_{sd} + V_{sq} i_{sq} \\ Q_s = V_{sq} i_{sd} - V_{sd} i_{sq} \end{cases} \quad (12)$$

$$\begin{cases} P_r = V_{rd} i_{rd} + V_{rq} i_{rq} \\ Q_r = V_{rq} i_{rd} - V_{rd} i_{rq} \end{cases} \quad (13)$$

The DFIG model is presented in synchronous dq reference frame where the d-axis is aligned with the stator flux linkage vector φ_s, and then, $(\varphi_{sq} = 0,\ \varphi_{sd} = \varphi_s)$ [13, 19]. In addition, considering that the resistance of the stator winding (R_s) is neglected and the grid is supposed stable with voltage v_s and synchronous angular frequency (ω_s) constant what implies $\varphi_{sd} = cst$, the voltage and the flux equations of the stator windings can be simplified in steady state as [17-21]:

$$\begin{cases} V_{sd} = \frac{d\varphi_{sd}}{dt} = 0 \\ V_{sq} = \omega_s . \varphi_{sd} = V_s \end{cases} \quad (14)$$

Hence, the relationship between the stator and rotor currents can be written as follows:

$$\begin{cases} i_{sd} = \frac{\varphi_s}{L_s} - \frac{L_m}{L_s} i_{rd} \\ i_{sq} = -\frac{L_m}{L_s} i_{rq} \end{cases} \quad (15)$$

From the equations (11) and (15), we can write:

$$\begin{cases} \varphi_{rd} = \left(L_r - \frac{M^2}{L_s}\right) i_{rd} + \frac{M\, V_s}{\omega_s L_s} \\ \varphi_{rq} = \left(L_r - \frac{M^2}{L_s}\right) i_{rq} \end{cases} \quad (16)$$

By replacing the equations (14), (16) in (8), (9) the stator and rotor voltages are then simplified to:

$$\begin{cases} V_{sd} = \frac{R_s}{L_s} \varphi_{sd} - \frac{R_s}{L_s} L_m i_{rd} \\ V_{sq} = -\frac{R_s}{L_s} L_m i_{rq} + \omega_s \varphi_{sd} \end{cases} \quad (17)$$

$$\begin{cases} V_{rd} = R_r i_{rd} + \sigma . L_r \frac{di_{rd}}{dt} + e_{rd} \\ V_{rq} = R_r i_{rq} + \sigma . L_r \frac{di_{rq}}{dt} + e_{rq} + e_\varphi \end{cases} \quad (18)$$

Where:

$$\begin{cases} e_{rd} = -\sigma . L_r . \omega_r . i_{rq} \\ e_{rq} = \sigma . L_r . \omega_r . i_{rd} \\ e_\varphi = \omega_r . \frac{M}{L_s} . \varphi_{sd} \\ \sigma = 1 - \left(\frac{M}{\sqrt{L_s L_r}}\right)^2 \end{cases} \quad (19)$$

By replacing (14), (15) in (12), (13), the equations below are expressed:

$$\begin{cases} P_s = -\frac{V_s . M}{L_s} . i_{rq} \\ Q_s = \frac{V_s^2}{L_s \omega_s} - \frac{M . V_s}{L_s} . i_{rd} \\ P_r = g . \frac{V_s . M}{L_s} . i_{rq} \\ Q_r = g . \frac{V_s . M}{L_s} . i_{rd} \end{cases} \quad (20)$$

The electromagnetic torque is as follows [16]:

$$T_{em} = -P . \frac{M}{L_s} \varphi_{sd} . i_{rq} \quad (21)$$

3. Wind Turbine Control System

In this section two control loops are presented: control loop of the electric generator via the rotor side converter and control loop of the aeroturbine without speed control that provides the reference inputs of the first loop. And second, to design a Fuzzy-PI controller in order to control active and reactive power. As seen in Fig. 3, the control loops will be considered separately.

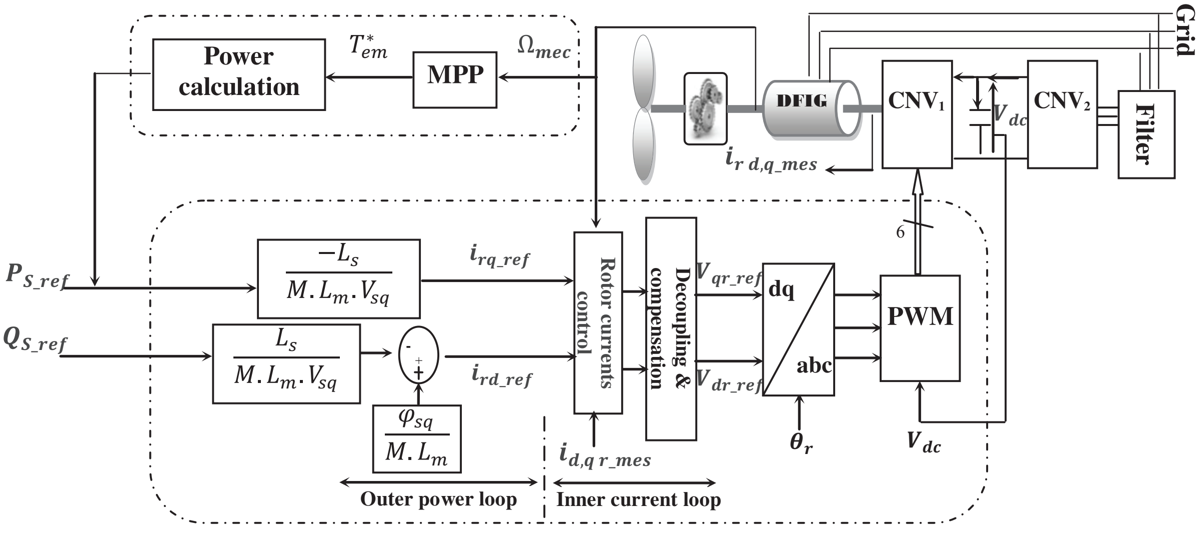

Fig. 3. Block diagram of the wind control system

3.1. MPP Control

The control system of DFIG wind turbine assures the variable speed operation that maximizes the output power for a wide range of wind speeds. The power extracted from the wind is maximized when the rotor speed is such that the power coefficient is optimal C_{popt}. Therefore, we must set the tip speed ratio on its optimal value λ_{opt}, so that turbine blade can capture the maximum of the wind power. The electromagnetic torque reference determined by MPP control power is thus expressed by the following equation [22, 23]:

$$T^*_{em} = \frac{C_{popt}.\rho.\pi.R^5}{2.G^3.\lambda^3_{opt}}.\Omega^2_m \tag{22}$$

3.2. Rotor side Converter Control CNV1

The rotor side converter CNV1 permits to control active and reactive powers produced by the DFIG. It is controlled by acting on the direct and quadrature components of the rotor voltage. It enables the decoupled control of active and reactive powers. Furthermore, equation (20) and (21) demonstrate that the electromagnetic torque and the stator reactive power can be controlled by means of the DFIG current i_{rq} and i_{rd} respectively. The model of DFIG in d-q reference frame with stator field orientation shows that the rotor currents can be controlled independently. The reference rotor currents i_{rd_ref} and i_{rq_ref} are given by:

$$\begin{cases} i_{rd\_ref} = \frac{\varphi_{sd}}{M} - \frac{L_s}{M.V_{sq}}.Q_{s\_ref} \\ i_{rq\_ref} = -\frac{L_s}{M.P.\varphi_{sd}}.T^*_{em} \end{cases} \tag{23}$$

4. Synthesis of PI and Adaptive Fuzzy PI Controllers

The synthesis of PI controller and the combination between the fuzzy logic and PI controller, which PI parameters controller can be adjusted by an adaptive mechanism based on a fuzzy inference system are presented in this section.

4.1. PI Synthesis

The transfer function of the open loop (TFOL) including the regulator is given by:

$$TFOL = \frac{S+\frac{k_i}{k_p}}{\frac{S}{k_p}} \cdot \frac{\frac{1}{\sigma.l_r}}{\frac{R_r}{\sigma.l_r}+S} \tag{24}$$

In the aim to compensate the constant of the time of system corresponding to the unfavorable pole from the viewpoint of the stability we can write:

$$S+\frac{k_i}{k_p}=\frac{R_r}{\sigma.l_r}+S \tag{25}$$

where: $\frac{k_i}{k_p}=\frac{R_r}{\sigma.l_r}$

If the poles are perfectly compensated we can write:

$$TFOL = \frac{k_p}{S}.\frac{1}{\sigma.l_r} \tag{26}$$

The transfer function in closed loop (TFCL) can be written as the following:

$$TFCL = \frac{1}{1+S.t_r} \tag{27}$$

Therefore:

$$t_r=\frac{\sigma l_r}{k_p} \to k_p = \frac{\sigma l_r}{t_r} \tag{28}$$

Of the (25) and (28) equation we have:

$$k_i = \frac{R_r}{\sigma l_r}.\frac{\sigma l_r}{t_r} \to \begin{cases} k_p = \frac{\sigma l_r}{t_r} \\ k_i = \frac{R_r}{t_r} \end{cases} \tag{29}$$

4.2. Design of Adaptive Fuzzy Gain Scheduling of PI Controller

In this work, our objective is to improve the system performances as precision, stability, rapidity and robustness. To answer these requires, we are interested to develop a control strategy based on the online adaptation of the PI controller parameters by the fuzzy logic technique. The adaptive fuzzy gain scheduling of PI controller (AFGS-PI) in a predefined way allows the use this controller for the nonlinear systems control [24, 25]. The AFGS-PI is used to control the electromagnetic torque and the stator reactive power by means of the DFIG current i_{rq} and i_{rd} respectively. Fig.4 show the block diagram of the adaptive fuzzy gain scheduler where the inputs and the outputs of the AFGPI are Ei_{r-dq}, dEi_{r-dq} and K'_{p_dq}, K'_{i_dq} respectively.

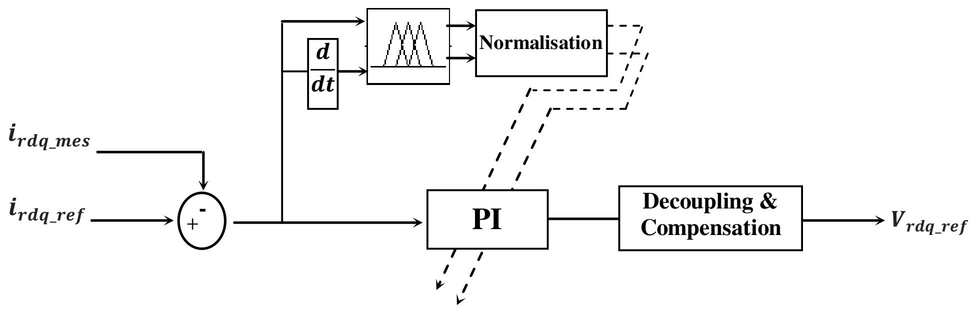

Fig.4. Block diagram of the adaptive fuzzy gain scheduler

The normalization PI parameters are given by [24-27]:

$$K_p' = \frac{K_p - K_{pmin}}{K_{pmax} - K_{pmin}} \quad (30)$$

$$K_i' = \frac{K_i - K_{imin}}{K_{imax} - K_{imin}} \quad (31)$$

Figures 5 and 6 show the fuzzy sets and corresponding triangular membership function (MF) of the fuzzy variables. The fuzzy sets are defined as follows: ZE=zero, PS=Positive Small, PM=Positive Medium, PB=Positive Big, NB= Negative Big. Fuzzy control rule database consists of series "IF-AND-THEN" fuzzy logic condition sentences.

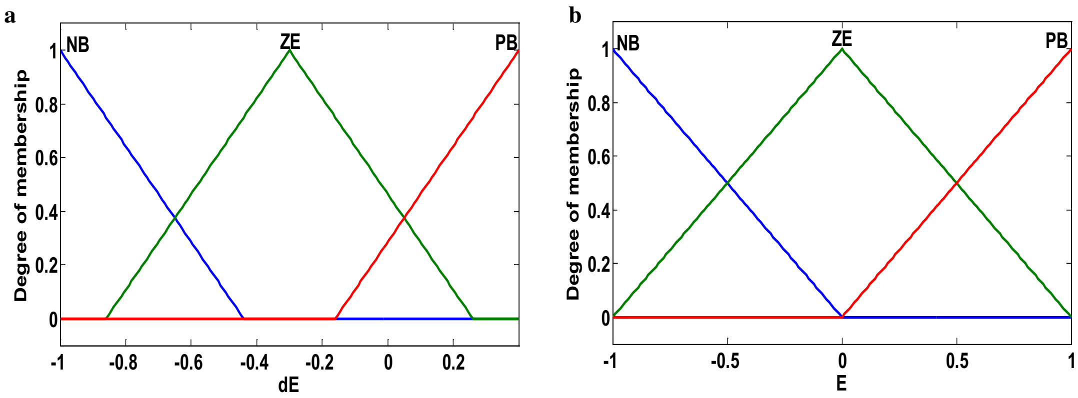

Fig. 5. (a, b) Error and variation error membership functions

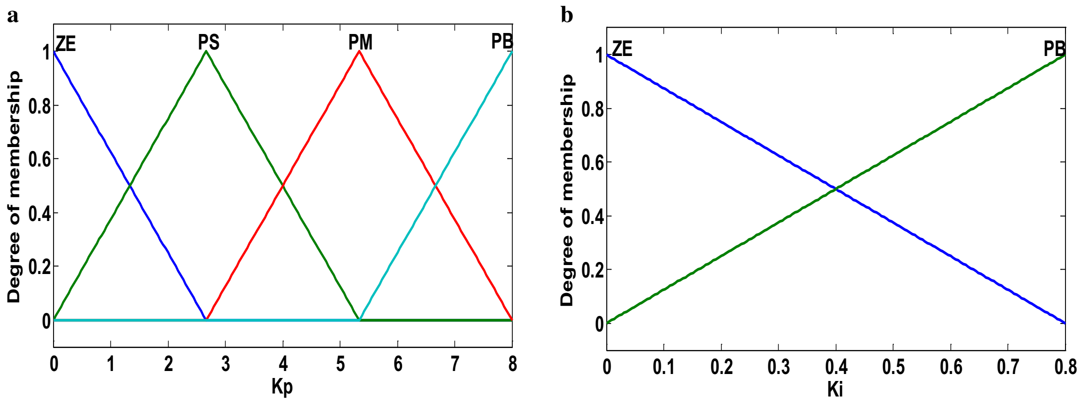

Fig. 6. (a, b) K_p' and K_i' membership functions

Tab. 1 show the tuning rules for K_p' and K_i'.

Table 1. Fuzzy rules base for computing K_p'/K_i'.

E/dE	NB K_p'/K_i'	ZE K_p'/K_i'	PB K_p'/K_i'
NB	ZE/ NB	ZE/ PB	ZE/ PB
ZE	PB/ ZE	PS/ PB	PB/ ZE
PB	ZE/ PB	PM/ PB	ZE/ PB

A.1. Stability

The system relative stability is measured by the margin phase (φ°) which corresponds to a gain unit ($|G(S)| = 1$):

$$\varphi^{\circ} = 180° + \arg(G_{OL}(j\omega_G)) \quad (32)$$

The system before correction has a margin phase φ° =90° for ω_G = 3070rd/s with a margin gain $M_{dB} = 0$.

$$M_{dB} = 20\, log|G_{BO}| = 20\, log\left({}^{1}/_{R_r}\right) - 20\, log\sqrt{\left(\left(\frac{\sigma L_r \omega}{R_r}\right)^2 + 1\right)} \quad (33)$$

The pulsation of cut is given by:

$$\omega_c = \frac{1}{T_i} = 55.8659 \quad (34)$$

With: $T_i = \frac{K_p}{K_i} = \frac{\sigma L_r}{R_r}$

Therefore, controller PI will be placed at the pulsation of cut ω_c=55.8659. In this case the corrected system has always a phase margin equal to $\frac{\pi}{2}$ due to integral actions of PI controller.

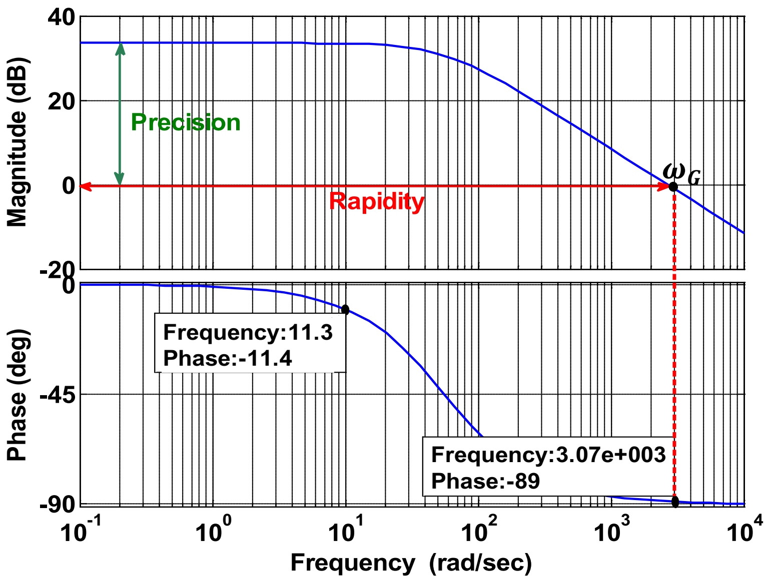

Fig. 7. Block diagram of the system before correction in bode plan

Pressing the harmonic response of the uncorrected system in the Bode plan (see Fig.7), we find that the PI controller can be placed at the pulsation ω_c forward of the pulsation ω_G = 3070rd/s so that the positive dephasing will be effective before the resonance pulsation of the uncorrected system, but without reducing the phase margin to avoid degrading the stability of the closed loop system or destabilize it completely. Finally, we can write:

$$\begin{cases} 11.3 \leq \omega_c \leq 3070 \\ 0.008 \leq T_i \leq 3.257 \end{cases} \quad (35)$$

From the previous equation, we can determine the universe of discourse parameters of : K_p' and K_i'.

A.2. Robustness

In the aim to test the robustness of the two controllers, the value of parameters has been changed as follows:

- variation of the rotor resistance Rr (+50%);
- variation of the stator, rotor and mutual self inductances (+20%).

5. Simulation and interpretation

In this work, we mainly aim to develop the decoupling method between active and reactive powers and improve not only the system performances but also to keep its stability. The system parameters, MPP control and controller gains are given in Appendix A and B, respectively. For this purpose, the robustness evaluation of the adaptive fuzzy gain scheduling of proportional integral controller was carried out by considering parametric variation, namely: rotor resistance, stator, rotor and mutual self inductances using MATLAB/Simulink environment. Fig.8 shows clearly that the measured rotor and stator current components, active and reactive powers of the DFIG follow respectively their references according to table 2 where the nominal parameters are given in table 3 of the appendix A. However, for the case of the PI controller, they present the discrepancies at the changes moments of their reference values. As well as at changing the “d” component current. But, these discrepancies do not occur in the case of the AFGPI controller (see Fig.8). This is obviously visible at the right of the presented zooms figures. To test the robustness system proposed under the influence of parameter variations, the simulation results are shown in Fig.9. It is noticed that the discrepancies and the overshoot (D) between the references and the real value are important, and that the response times (tr) are slower for PI controller compared to AFGPI controller. Under these conditions, the synthesis of this analysis is summarized in the following table.

Table 4. Response time and overshoot of PI and AFGPI controllers with parametric variation

		D_1/tr_1	D_2/tr_2
PI controller	Ird	281 / 0.0255	493.5 / 0.0249
	Isd	-232.3 / 0.025	417.6 / 0.0252
	Qs	-2.77×10^5 / 0.0248	4.99×10^5 / 0.0254
	Qr	1825 / 0.0256	-3261 / 0.0251
AFGPI controller	Ird	46 / 0.0079	108.7 / 0.0134
	Isd	-38.7 / 0.0068	95.8 / 0.0134
	Qs	-4.6×10^4 / 0.0099	11.59×10^4 / 0.0114
	Qr	300 / 0.0082	-735 / 0.0119

a

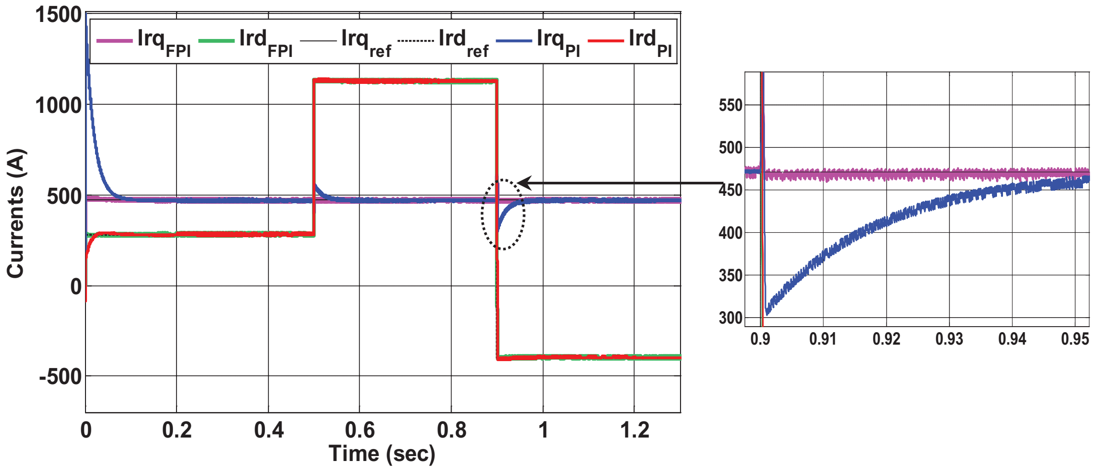

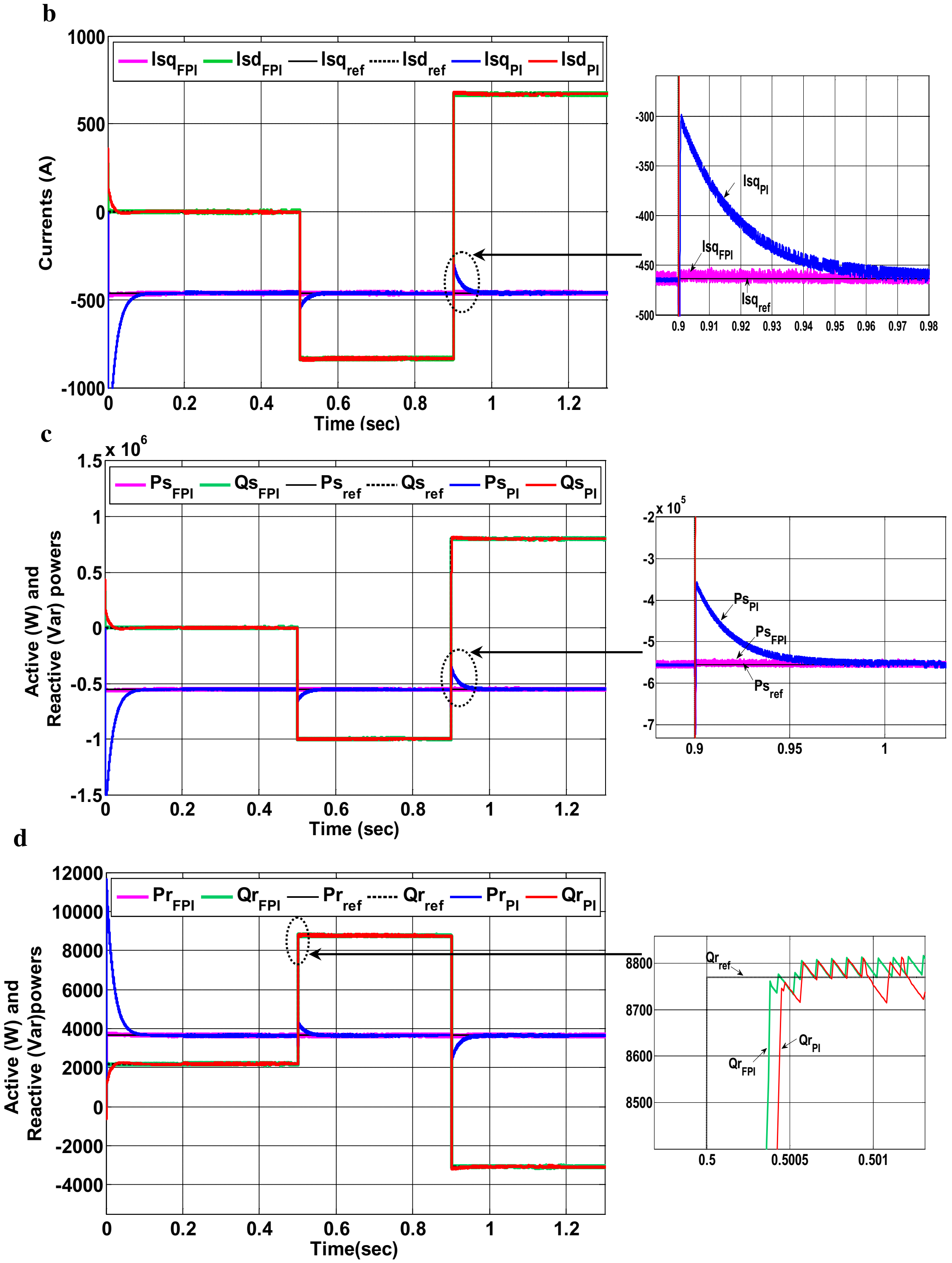

Fig. 8. (a, b) currents d-q axis; (c, d) active and reactive powers

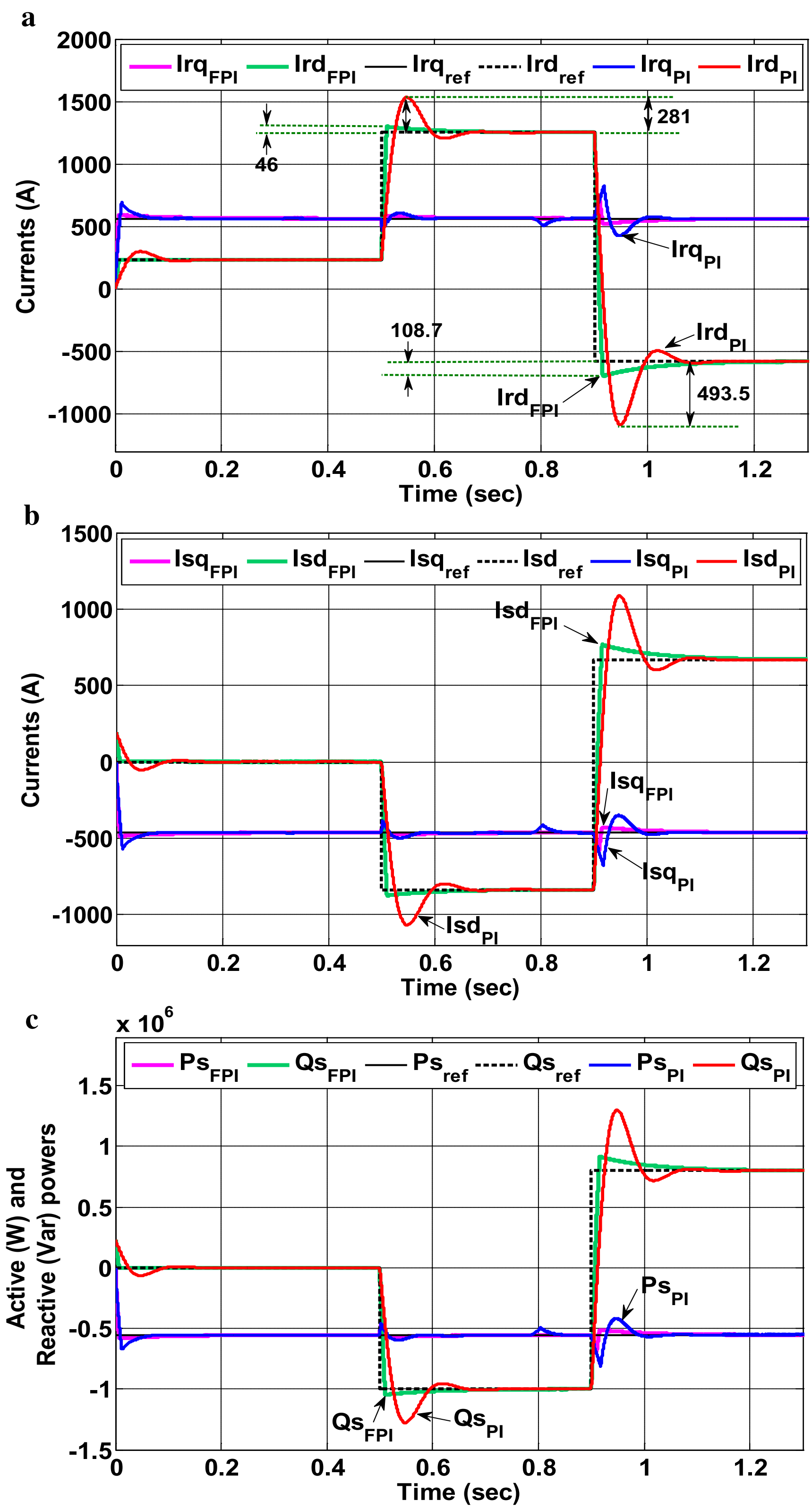
a
Irq_FPI Ird_FPI Irq_ref Ird_ref Irq_PI Ird_PI
Currents (A)
Time (sec)
46
281
108.7
493.5
Irq_PI
Ird_PI
Ird_FPI
b
Isq_FPI Isd_FPI Isq_ref Isd_ref Isq_PI Isd_PI
Currents (A)
Time (sec)
Isd_FPI
Isq_FPI
Isq_PI
Isd_PI
c
x 10^6
Ps_FPI Qs_FPI Ps_ref Qs_ref Ps_PI Qs_PI
Active (W) and Reactive (Var) powers
Time (sec)
Ps_PI
Qs_FPI
Qs_PI

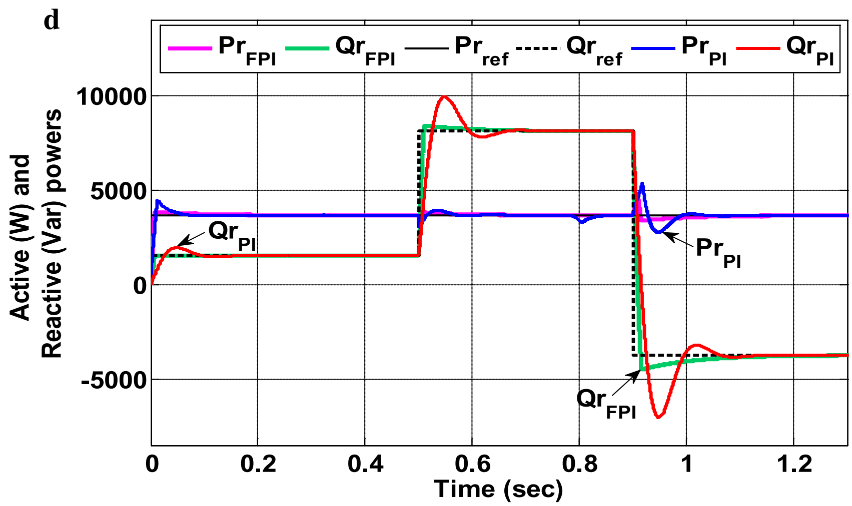

Fig. 9. (a, b) currents d-q axis and (c, d) active and reactive powers with parameters variation

6. Conclusion

In this paper, a powers control strategy for doubly fed induction generator which provides decoupled control of active and reactive power is presented. However, the fact of the control of these powers separately permits to adjust the power factor of the installation and in consequence obtain better performance. Therefore, adaptive fuzzy gain scheduling of proportional integral controller was developed. To achieve, our works are validated through simulation studies on a 1.5 MW DFIG wind generation system compared with conventional proportional integral current control design. The simulation results show the effect of parameters variation for the two controllers which explains that the PI controller regulating performances degrades with the variation of the parameters. On the other hand, adaptive fuzzy PI control assures better performances because when the operating condition of system changes, the PI parameters are adjusted by the collection of “IF-THEN” fuzzy rules while remaining insensible to the variations of the parameters. A good performance and robustness quality of AFGPI controller are shown in the simulation results using software Matlab/Simulink.

Appendix A.

Table 2. Operation Statues of the Simulated DFIG

Status	Time (sec)	Reactive power (MVar)
1	$0 < t \leq 0.5$	0
2	$0.5 < t \leq 0.9$	-1
3	$0.9 < t \leq 1.3$	0.8

Table 3. Font Simulated DFIG Wind Turbine Parameters

Rated power	1.5MW
Rotor diameter	35.25m
Gearbox ratio	90
Friction coefficient : f	0.0024
Moment of inertia : J	1000
Stator voltage/Frequency	690V/50Hz
$Rs\ /\ Rr$ (Ω)	0.012/0.021
$Lm/Lfs/Lfr$ (H)	0.0135/0.00020372/0.0001757
Number of pole pairs: p	2
M	1

Appendix B. MPP control & Controller gains

$$\begin{cases} \lambda_{opt} = 7.64. \\ C_{popt} = 0.45. \end{cases}$$

For the synthesis of the regulators we opted for the method of poles compensation (t_r= 0.05s);

$$K = \sigma * \frac{Lr}{t_r} = 0.0075$$

$$I = \frac{Rr}{t_r} = 0.42$$

References

[1] A. Susperregui, J. Jugo, I.Lizarraga, G. Tapia, ‘Automated Control of Doubly Fed Induction Generator Integrating Sensorless Parameter Eestimation and Grid Synchronization,’ Renewable Power Generation IET, v. 8, pp. 76-89, 2014.

[2] B.Shen, B. Mwinyiwiwa, Y. Zhang, B.T. Oo “Sensorless Maximum Power Point Tracking of Wind by DFIG Using Rotor Position Phase Lock Loop (PLL) ”, IEEE Transactions on Power Electronics, vol. 24, no. 4, April 2009

[3] S. Karimi, A. Gaillard, P. Poure, S. Saadate “FPGA-Based Real-Time Power Converter Failure Diagnosis for Wind Energy Conversion Systems”, IEEE Transactions on Industrial Electronics, vol. 55, no. 12, December 2008.

[4] M. Tazil, V. Kumar, R. C. Bansal, S. Kong, Z. Y. Dong, W. Freitas, H. D. Mathur, "Three-phase doubly fed induction generators: an overview," IET Electric Power Applications, vol. 4, no. 2, pp. 75-89, Feb. 2010.

[5] O. Anaya-Lara, N. Jenkins, J. Ekanayake, P. Cartwright, M.Hughes, “Wind energy generation: Modelling and control”, Chichester, UK: John Wiley & Sons, 2009.

[6] R. V. de Oliveira, J. A. Zamadei, C. H. Hossi, “Robust Tuning of the Control Loops of DFIG Wind Turbine Systems,” IEEE International Conference on Control Applications Part of 2011 IEEE Multi-Conference on Systems and Control Denver, CO, USA. Sep 28-30, 2011.

[7] E. Tremblay, S. Atayde, A. Chandra, “Direct Power Control of a DFIG-based WECS with Active Filter Capabilities,” IEEE Electrical Power & Energy Conference, 2009.

[8] B. Beltran, M. E. H. Benbouzid, and T. Ahmed-Ali, ‘Second-Order Sliding Mode Control of a Doubly Fed Induction Generator Driven Wind Turbine,’ IEEE Trans on Energy Conversion, v. 27, no. 2, pp. 261-269, 2012.

[9] J. A. Baroudi, V. Dinavahi, A. M. Knight, “A review of power converter topologies for wind generators”, Renewable Energy, vol. 32, no. 14, pp. 2369-2385, Nov. 2007.

[10] M. J. Zandzadeh, A.Vahedi, “Modeling and improvement of direct power control of DFIG under unbalanced grid voltage condition,” Electrical Power and Energy Systems, vol. 59, pp. 58–65, July. 2014.

[11] B. Beltran, al. Sliding, “Mode power control of variable speed wind energy conversion systems,” IEEE Trans. Energy Conversion, vol. 23, no. 2, pp. 551-558, 2008.

[12] D. B. Fernando, Hrnan De Battista, J. M. Ricardo, “Wind Turbine Control Systems Advances in Industrial Control Series,” Springer.

[13] O. Barambones, Jose M. Gonzalez de Durana, E. Kremers, “Adaptive robust control to maximizing the power generation of a variable speed wind turbine,” International Conference on Renewable Energy Research and Applications Madrid, Spain, 20-23 October 2013, IEEE, ICRERA, 2013.

[14] S. Abdeddaim, A. Betka, “Optimal tracking and robust power control of the DFIG wind turbine,” Electrical Power and Energy Systems, vol. 49, pp. 234 – 242, 2013.

[15] E. S. Abdin, W. Xu, “Control design and Dynamic Performance Analysis of a Wind Turbine Induction Generator Unit,” IEEE Trans on Energy Conversion , vol. 15, no. 1, March. 2000.

[16] A. Gaillard, “Wind system based on the DFIG: contribution to the study of the quality of the electric energy and the continuity of service,” Doct. thesis, Henri Poincare University, Nancy-I, France, April. 2010.

[17] B. Boukhezzar, H. Siguerdidjane, "Nonlinear control with wind estimation of a DFIG variable speed wind turbine for power capture optimization", Energy Conversion and Management, vol. 50, pp. 885–892, February. 2009.

[18] C. Belfedal, S. Gherbi, M. Sedraoui, S. Moreau, G. Champenois, T. Allaoui, M.A. Denai, "Robust control of doubly feed induction generator for stand-alone applications," Electric Power Systems Research, vol. 80, pp. 230–239, 2010.

[19] Ahmed M. Kassem, Khaled M. Hasaneen, Ali M. Yousef, "Dynamic modeling and robust power control of DFIG driven by wind turbine at infinite grid," Electrical Power and Energy Systems, vol. 44, pp. 375-382, 2013.

[20] M. Zamanifar, B. Fani, M.E.H. Golshan, H.R. Karshenas, "Dynamic modeling and optimal control of DFIG wind energy systemsusing DFT and NSGA-II," Electric Power Systems Research, vol. 108, pp. 50– 58, 2014.

[21] T. Ghennam1, E.M.Berkouk2, B.François3, "Modeling and Control of a Doubly Fed Induction Generator (DFIG) Based Wind Conversion System," IEEE International conference on power engineering, energy and electrical drives (POWERENG), March 18-20, 2009.

[22] L.M. Fernandez, C.A. Garcia, F. Jurado, "Comparative study on the performance of control systems for doubly fed induction generator (DFIG) wind turbines operating with power regulation," Energy, vol. 33, pp. 1438– 1452, 2008.

[23] M. Boutoubat, L. Mokrani, M. Machmoum, "Control of a wind energy conversion system equipped by a DFIG for active power generation and power quality improvement," Renewable Energy, vol. 50, pp. 378-386, 2013.

[24] Zhen-Yu Zhao, M. Tomizuka, S. Isaka, 'Fuzzy Gain Scheduling of PID Controllers,' IEEE Trans. on Systems, Man. and Cybernetics, vol. 23, no . 5, 1993.

[25] P. Viljamaa, "Fuzzy Gain Scheduling and Tuning of Multivariable Fuzzy Control-Methods of Computing in Control Systems," Technologic doctoral thesis, Temper University of technology, Finland, 2000.

[26] A. Selk Ghafari A. Alasty, 'Design and Real-Time Experimental Implementation of Gain Scheduling PID Fuzzy Controller for Hybrid Stepper Motor in Micro-Step Operation,' Mechatronics, 2004. ICM '04. Proceedings of the IEEE International Conference on , pp. 421 – 426, 2004.

[27] B. Hamane, M. Benghanem, A. M. Bouzid, A. Belabbes, M. Bouhamida, A. Draouf, "Control for Variable Speed Wind Turbine Driving a Doubly Fed Induction Generator using Fuzzy-PI Control," Energy Procedia, vol. 18, pp. 476 – 485, 2012.